Phase-gradient CsPbBr₃ perovskite structure

© *E.I. Battalova, S.S. Kharintsev*

Kazan Federal University, Kazan, Tatarstan, Russia

e-mail: elibattalova@kpfu.ru

We introduce a strategy to develop multiple-phase structure of inorganic lead halide perovskite $CsPbBr_3$. The method is based on local optical heating, which allows the creation of strong temperature gradients. Using Raman spectroscopy, it was determined that such gradients induce a distribution of phase transitions within the perovskite crystal. We show that such gradients lead to perovskite multiple-phase structure.

The development of semiconductor nanoelectronics is inextricably linked with the development of new materials. In recent years, inorganic halide perovskites $CsPbX_3$(X-Cl, Br, I) have attracted wide interest for photonic and optoelectronic applications [1–3]. The crystal lattice of $CsPbX_3$ is a three-dimensional network of $[PbX]_6^{4-}$ octahedra with common sites, in the space between which there are Cs^+ ions. The symmetry of the perovskite crystal lattice can change significantly during phase transitions, when internal stresses arise and structural defects are formed due to tilts and distortions of the octahedra. Typically, the crystalline phases of inorganic halide perovskites differ in their band gaps. This leads to the migration of charge carriers from regions with a larger band gap to regions with a smaller band gap, which is most pronounced near areas of phase transitions [4,5]. The accumulation of free charge carriers in the phase region with a smaller band gap increases the probability of radiative electron-hole recombination, which increases the efficiency of optical processes (photoluminescence, Raman scattering, etc.) [6]. This phenomenon can be used to actively tune the optoelectronic properties of semiconductors, in particular, to create dynamically controlled multiphase heterostructures.

This work discusses the concept of creating a heterostructure consisting of several crystalline phases of inorganic halide perovskite $CsPbBr_3$. Depending on the mutual orientation of the octahedra, the structure of $CsPbBr_3$ can be stable in three phases: orthorhombic (Pnma), tetragonal (P4/mbm) and cubic (Pm3m) [7]. A thermoplasmonic metasurface is used to create a multiphase structure. The thermoplasmonic metasurface is a two-dimensional array of nanoscale TiN/Si structures (Fig. 1, *a*). Each nanostructure looks like a silicon column, on the top surface of which a thin layer of titanium nitride (TiN) is placed. When illuminated with focused laser light (633 nm, 16 mW, NA = 0.7), a plasmon resonance appears in the TiN nanostructure, leading to its strong heating up to 1000 K. The maximum heating temperature of the nanostructure is determined by the intensity of the incident radiation.

In this case, the silicon structure acts as a channel for heat removal [8,9]. Figure 1, *a* shows an atomic-force microscopy (AFM) image of a $CsPbBr_3$ microcrystal on a metasurface. A $CsPbBr_3$ perovskite microcrystal in the form of a platform with linear dimensions $10 \times 14 \times 1\,\mu m^3$ was placed on a thermoplasmonic metasurface using a micromanipulator. Since $CsPbBr_3$ has low thermal conductivity $(0.42\,Wm^{-1}K^{-1})$, and phase transitions occur at relatively high temperatures (88°C for the Pnma-P4/mbm transition and 130°C for the P4/mbm-Pm3m transition), inside the crystal on the metasurface strong temperature gradients may arise (Fig. 1, *b*) [8,10]. Such temperature gradients should lead to a phase distribution inside the perovskite crystal that depends on the distance to the heated plasmonic nanostructure. To determine the heating temperature of the crystal, the method of Raman light scattering thermometry was used. It is based on the dependence of the Raman scattering line shift on temperature. The analytical form of this dependence is presented in work [11]. Using RS thermometry, a temperature map was constructed from the shift of the line of crystalline silicon $(521\,cm^{-1})$ (Fig. 1, *b*). According to the obtained map, under the influence of incident light, nanostructures of a thermoplasmonic metasurface can be heated to temperatures of the order of 500 K, which is sufficient to activate all structural phase transitions in $CsPbBr_3$. To determine phase transitions, the temperature dependence of the intensity of the transverse optical single-phonon mode $127\,cm^{-1}$ was studied. This mode corresponds to the stretching vibrations of the Pb-Br bond, and its intensity provides information about the mutual orientation of the $[PbBr]_6^{4-}$ [12] octahedra. Figure 2, *a* shows the dependence of the intensity of the TO mode $(127\,cm^{-1})$ on temperature when heated using a temperature table. It experiences two extremes corresponding to the phase transitions $\gamma \rightarrow \beta$ (361 K) and $\beta \rightarrow \alpha$ (403 K). In the region of the tetragonal phase, there is a decrease in the intensity of the RS line with increasing temperature. This behavior of the line intensity can be
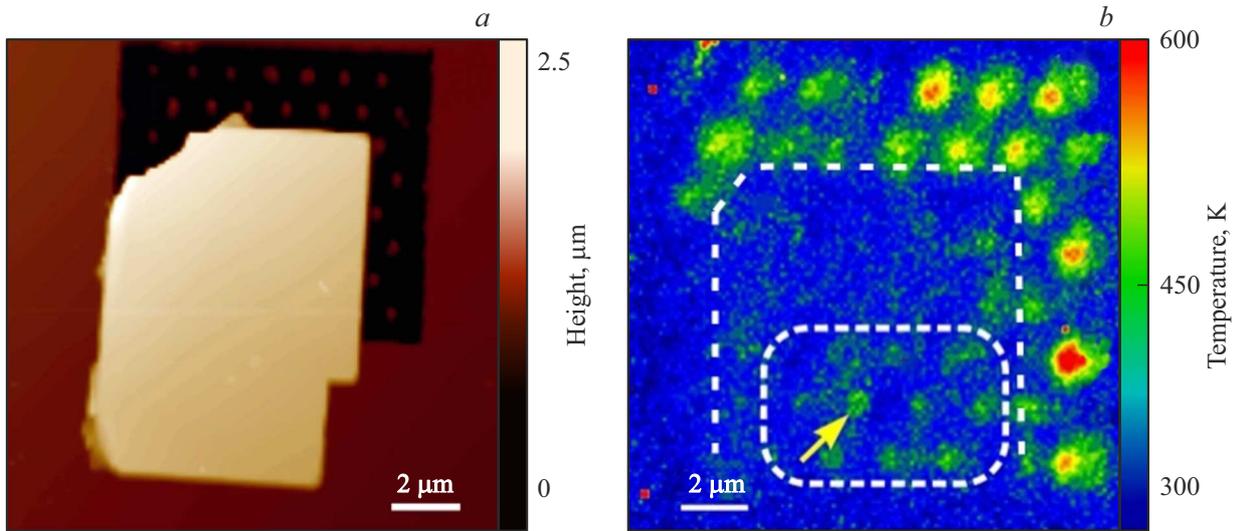
Figure 1. *a* — AFM image of a CsPbBr$_3$ crystal on the metasurface, *b* — temperature map obtained at a pumping intensity of 3.5 MW/cm^2. The color indicates the temperature of each individual nanostructure.
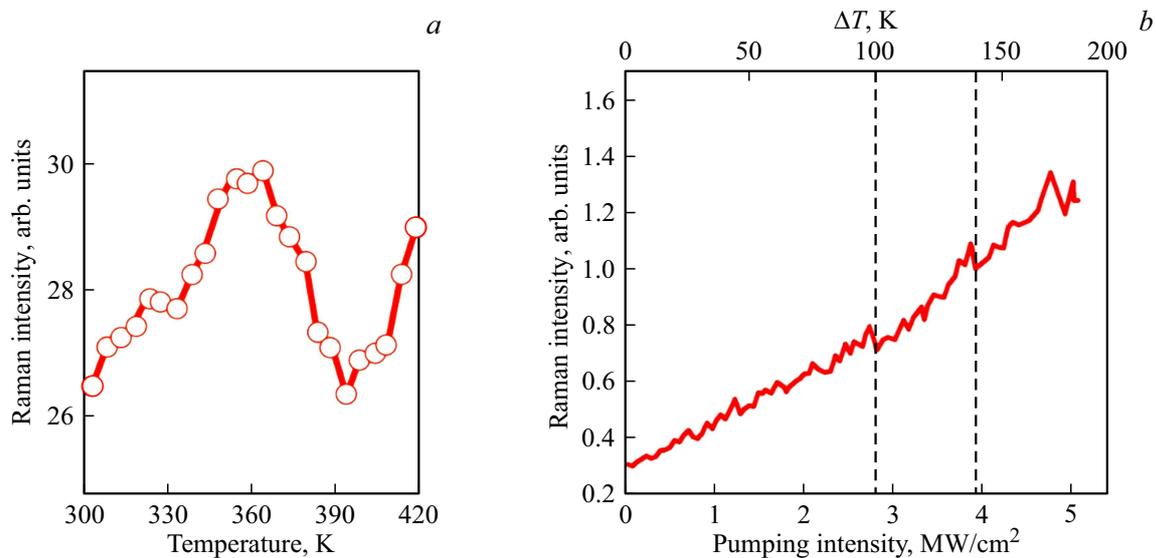
Figure 2. Temperature dependence of the intensity of Raman light scattering of a CsPbBr$_3$ microcrystal for the 127 cm^{-1} TO mode when heated using a temperature stage (*a*) or a metasurface (*b*).

caused by an increase in the band gap and a decrease in free charge carriers in the valence band [5,6]. Meanwhile, there is an opposite trend in the temperature dependences of the RS line intensities in the α phase and the γ phase. This can be explained by thermal volumetric expansion of the lattice, accompanied by distortions of the $[PbBr6]_6^{4-}$ [5] octahedra. Figure 2, *b* shows the change in the intensity of the 127 cm^{-1} line with a change in the temperature of the plasmonic nanostructure. Vertical dashed lines mark the position of local maxima. The first maximum is located near the transition temperature from the γ phase to the β phase. It indicates the beginning of phase transitions between the orthorhombic phase and the tetragonal one. A further increase in the temperature of the plasmonic nanostructure

shifts the region of the β phase deeper into the crystal volume. When the temperature changes by 130 K, another small maximum in the Raman light scattering intensity indicates the formation of the α phase in the immediate vicinity of the top surface of the plasmonic nanostructure.

There is a physical model below for the analysis of the dependence presented in Fig. 2, *b*. The mechanism of formation of the multiphase structure CsPbBr$_3$ is schematically presented in Fig. 3, *a*. It shows that the temperature gradient induces phase transitions in the direction perpendicular to the surface of the nanostructure. The RS intensity signal from such a multiphase structure represents the combined signal from all phases within the focal spot. The cumulative RS intensity ($\tilde{I}_R$) is introduced to describe this signal. It
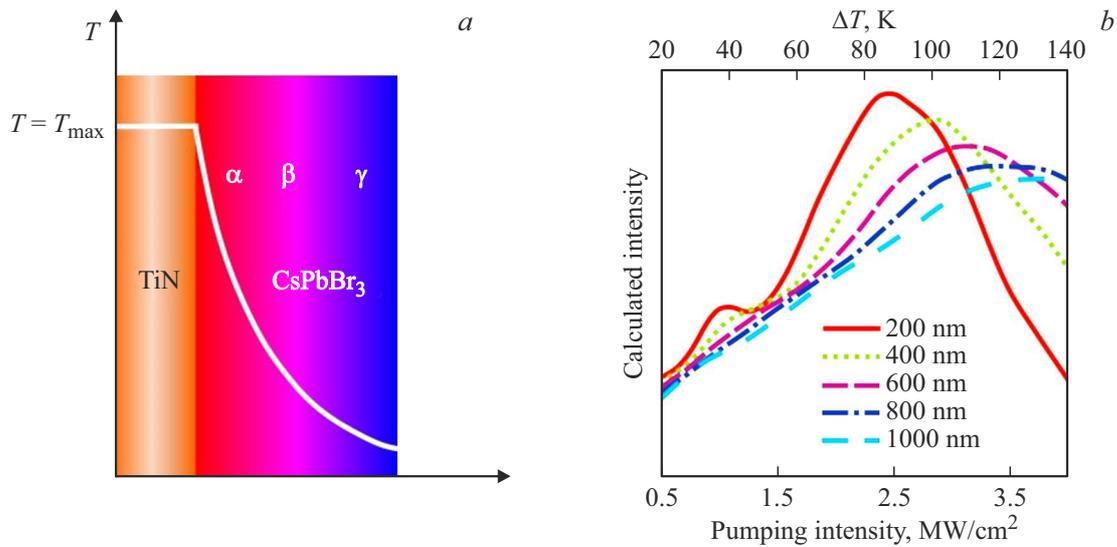
Figure 3. Schematic illustration of the formation of the multiphase structure of CsPbBr$_3$ under the influence of a strong temperature gradient (*a*); the result of simulating the cumulative intensity of the RS signal of crystals of different thicknesses (*b*).

reflects the process of formation of a multiphase perovskite structure when the temperature $T_m(0)$ of the plasmonic nanostructure changes. If the temperature gradient inside the perovskite crystal is formed along the z axis according to a power law of the form $T_m(z) = T_m(0)|z|^{-\mu}$ (Fig. 3, *a*), then the dependence of the RS signal intensity on temperature will be a convolution of two functions:

$$\langle I(z) \rangle = \int_{T_0}^{T_m(z)} K_z[T_m(z) - T]I_R(T)dT, \quad (1)$$

where $K_z(T)$ — kernel of the integral determined by the phase distribution inside the perovskite crystal, T_0 — ambient temperature. The distribution of phases inside the crystal depends on the type and concentration of defects, since structural defects significantly affect the kinetics of phase transitions [13]. In the general case, the cumulative intensity of the Raman signal is obtained by averaging (1) over the crystal thickness Δz:

$$\tilde{I}_R = \int_0^{\Delta z} \langle I(z) \rangle dz. \quad (2)$$

Figure 3, *b* shows the results of simulating the dependence of I_R on I_0 for different thicknesses of the perovskite crystal. For very thin crystals (< 200 nm), the temperature dependence of the intensity of the Raman light scattering signal repeats the behavior of the curve shown in Fig. 2, *a*). For thicker crystals, several crystalline phases can contribute to the observed Raman light scattering signal. In this case, a local maximum appears against the background of a monotonically increasing RS signal, which indicates the formation and growth of a two-phase structure (γ and β) in the direction of the z axis.

Thus, this work demonstrates a method for creating a multiphase structure of semiconductors using the example of inorganic halide perovskites CsPbBr$_3$. This work proposes a method that allows one to tune the phase composition of semiconductors using local optical heating. A physical model has been constructed to explain the mechanism of formation of the multiphase structure CsPbBr$_3$. Such multiphase semiconductor systems open up the possibility of creating a new class of optoelectronic devices with improved efficiency.

Funding

Conflict of interest

The authors declare that they have no conflict of interest.

References

[1] S.D. Stranks, G.E. Eperon, G. Grancini, C. Menelaou, M.J.P. Alcocer, T. Leijtens, L.M. Herz, A. Petrozza, H.J. Snaith. Science, **342** (6156), 341 (2013). DOI: 10.1126/science.1243982

[2] M. Ahmadi, T. Wu, B. Hu. Adv. Mater., **29** (41), 1605254 (2017). DOI: 10.1002/adma.201605242

[3] J. Chen, H. Xiang, J. Wang, R. Wang, Y. Li, Q. Shan, X. Xu, Y. Dong, C. Wei, H. Zeng. ACS Nano, **15** (11), 17150 (2021). DOI: 10.1021/acsnano.1c06849

[4] G. Mannino, I. Deretzis, E. Smecca, A. La Magna, A. Alberti, D. Ceratti, D. Cahen. J. Phys. Chem. Lett., **11** (7), 2490 (2020). DOI: 10.1021/acs.jpclett.0c00295

[5] H.M. Ghaithan, Z.A. Alahmed, S.M.H. Qaid, M. Hezam, A.S. Aldwayyan. ACS Omega, **5** (13), 7468 (2020). DOI: 10.1021/acsomega.0c00197

[6] A. Dobrovolsky, A. Merdasa, E.L. Unger, A. Yartsev, I.G. Scheblykin. Nat. Commun., **8**, 34 (2017). DOI: 10.1038/s41467-017-00058-w

[7] A. Alaei, A. Circelli, Y. Yuan, Y. Yang, S. S. Lee. Mater. Adv., **2** (1), 47 (2021). DOI: 10.1039/d0ma00643b

[8] S.S. Kharintsev, A.V. Kharitonov, E.A. Chernykh, A.M. Alekseev, N.A. Filippov, S.G. Kazarian. Nanoscale, **14** (33), 12117 (2022). DOI: 10.1039/D2NR03015B

[9] G. Baffou, R. Quidant, F.J.G. de Abajo. ACS Nano, **4** (2), 709 (2010). DOI: 10.1021/nn901144d

[10] W. Lee, H. Li, A.B. Wong, D. Zhang, M. Lai, Yi Yu, Q. Kong, E. Lin, J.J. Urban, J.C. Grossman, P. Yang. Proc. Natl. Acad. Sci. USA, **114** (33), 8693 (2017). DOI: 10.1073/pnas.1711744114

[11] T.R. Hart, R.L. Aggarwal, B. Lax. Phys. Rev. B, **1** (2), 638 (1970). DOI: 10.1103/PhysRevB.1.638

[12] Z. Zhao, M. Zhong, W. Zhou, Y. Peng, Y. Yin, D. Tang, B. Zou. J. Phys. Chem. C, **123** (41), 25349 (2019). DOI: 10.1021/acs.jpcc.9b06643

[13] A.G. Ambrok, E.V. Kalashnikov, S.A. Kukushkin. J. Appl. Phys., **91** (8), 4961 (2002). DOI: 10.1063/1.1445491

Translated by E.Potapova